A Pervasive Assessment of Motor Function: A Lightweight Grip Strength Tracking System

Sunghoon Ivan Lee, *Student Member, IEEE*, Hassan Ghasemzadeh, *Member, IEEE*, Bobak Jack Mortazavi, *Student Member, IEEE*, and Majid Sarrafzadeh, *Fellow, IEEE*

***Abstract*—With the growing cost associated with the diagnosis and treatment of chronic neuro-degenerative diseases, the design and development of portable monitoring systems becomes essential. Such portable systems will allow for early diagnosis of motor function ability and provide new insight into the physical characteristics of ailment condition. This paper introduces a highly mobile and inexpensive monitoring system to quantify upper-limb performance for patients with movement disorders. With respect to the data analysis, we first present an approach to quantify general motor performance using the introduced sensing hardware. Next, we propose an ailment-based analysis which employs a significant-feature identification algorithm to perform cross-patient data analysis and classification. The efficacy of the proposed framework is demonstrated using real data collected through a clinical trial. The results show that the system can be utilized as a preliminary diagnostic tool to inspect the level of hand-movement performance. The ailment-based analysis performs an intergroup comparison of physiological signals for cerebral vascular accident (CVA) patients, chronic inflammatory demyelinating polyneuropathy (CIDP) patients, and healthy individuals. The system can classify each patient group with an accuracy of up to 95.00% and 91.42% for CVA and CIDP, respectively.**

***Index Terms*—Ailment classification, grip strength tracking, movement disorders, pervasive medical system, upper limb deficits.**

I. Introduction

AILMENTS such as stroke [1], Parkinson's Disease (PD) [2], spinal cord injuries [3], and many other neuro-degenerative disorders are commonly associated with movement deficits, which affect the function of motor neurons and restrict the movements of the body such as those of the upper limbs, gait, and speech performance [4].

Currently, the available assessment methods for the progress of patients with associated ailments are based on human observations of motor performances (e.g., finger-to-nose test) [5], [6]. Clinical professionals use these measurements for preliminary scanning in order to diagnose ailments in early stage. The early detection of these ailments can dramatically reduce the risk of the severity of motor deficits [7].

Manuscript received August 6, 2012; revised December 7, 2012; accepted April 14, 2013. Date of publication May 16, 2013; date of current version November 12, 2013.

The authors are with the Department of Computer Science, University of California, Los Angeles, CA 90095 USA (e-mail: silee@cs.ucla.edu; hassan@cs.ucla.edu; bobakm@cs.ucla.edu; majid@cs.ucla.edu).

Color versions of one or more of the figures in this paper are available online at http://ieeexplore.ieee.org.

Digital Object Identifier 10.1109/JBHI.2013.2262833

Furthermore, medical treatments available for movement disorders are typically a combination of medication, surgical operation, and rehabilitation. These treatments are often evaluated by measuring the motor performance of the patients before and after the specific service (e.g., surgery), again, based on human observations. However, these methods suffer from the subjective nature of the measurements, which are often based on limited ordinal scales [6]. This subjectivity creates a need for quantitative assessment methods, such that the analysis of patients' motor performances can be made more accurate and objective [8].

Researchers have studied various methods to objectively quantify the level of upper limb movement. Among those methods, handgrip performance has been known as a simple, accurate, and economical bedside measurement of muscle function and the progression of the movement disorders [9]–[18]. The grip control is of extreme importance in performing fundamental daily activities such as eating, brushing teeth, and getting dressed. However, existing works often employ equipment that are either very large in size or extremely expensive. Moreover, they often lack in-depth analysis on patients' motor performance with respect to their ailment conditions.

Given the current standard of healthcare for movement disorder patients, there is a need for innovative technologies that 1) provide wearable and portable devices that can be used on a daily basis in many settings; 2) can be used for individuals' stratification so that such systems are applied on healthy individuals to potentially provide early alarming of any movement disorders; 3) quantify the level of severity of the specific disorder for a patient; and 4) provide insight on disease symptoms by specifying each abnormality/symptom in terms of signal-specific features.

This paper introduces a lightweight and inexpensive handgrip device that collects multidimensional sensory data associated with motor characteristics of individuals with upper limb deficits. Furthermore, a data analytic framework with associated algorithms for individuals' ailment classification, disease severity quantification, and specification of physical symptoms is discussed. The effectiveness of the proposed movement performance assessment framework is demonstrated through a dataset gathered in a clinical trial performed at St. Vincent Medical Center in Los Angeles, CA, USA.

II. Related Works

Many studies have examined handgrip performance in order to reflect the motor capacity of patients with movement disorders. The mechanisms used to investigate the handgrip performances can be divided into three broad categories: 1) assessment based on precision grip; 2) assessment based on maximum

voluntary contraction (MVC);[1] and 3) assessment based on force tracking tasks.

Assessment methods based on precision grip focus on simulating tasks involving precise muscle control such as lifting, holding, or transporting a small object (e.g., chopsticks or a pencil) [19]. In [9], authors utilize a force sensor embedded apparatus in order to investigate digit forces when an active and dynamic hand grasping movement is simulated. In [20], a device embedded with a force sensor and an accelerometer is used to assess finger strength. In [10], an instrumented glove was used to analyze finger movement of patients with subcortical stroke.

MVC-based assessment methods utilize various systems and devices to measure MVC. In [21], a simple dynamometer is used in order to measure the MVC as a measure of recovery and a prognostic indicator for patients with stroke. The system in [22] uses a vigorimeter, which measures the air pressure using a rubber bulb. Then, a few features of MVC are analyzed to reflect the disease progress over time. In [12], authors investigate the handgrip strength and endurance of healthy subjects and patients using a dynamometer, and conclude that handgrip strength and mobility for patients are strongly correlated. The system proposed in [13] uses instrumented objects that measure forces applied during tasks such as manipulating a book, or a fork.

Assessments based on force tracking tasks provide visual feedback of patients' hand performances, such that patients can control their grip force to minimize the difference between the target and the actual response [23]. The system proposed in this paper improves upon methods that fall within this category. The system in [23] and [14] utilizes various types of devices, such as a nippers pinch, spherical grip, lateral grip, and cylindrical grip, in order to capture the grip force. The system uses a sinusoidal and ramp waveform for the target. Two features are extracted in order to analyze the patients' motor performance: root mean square error and correlation between the target waveform and the user response. In [5], authors propose a handgrip device that measures forces generated by individual fingers using pressure sensors. In [24], authors utilize a grasping apparatus to capture grip forces, and provide a target waveform of a continuous and constant force level on a computer screen.

Most of the aforementioned works (i.e., [9], [10], [12], [13], [19]–[23], [25]) focus on introducing the developed handgrip devices using a simple metric to validate the effectiveness of those devices. Thus, these works often lack in-depth analysis of the data according to their ailment conditions. Furthermore, some of the devices such as those used in [9], [12], and [22]–[24] are either very large in size or extremely expensive.

III. System Architecture

The proposed system is composed of 1) the sensing hardware that contains a handgrip device equipped with a force sensor in order to collect the time-varying muscle controllability of patients; and 2) the software system that visualizes the examination and stores the results in the database. An overview of the proposed system is illustrated in Fig. 1.

[1]MVC defines the amount of force that a patient produces when she voluntarily grasps the handgrip device with maximum effort.

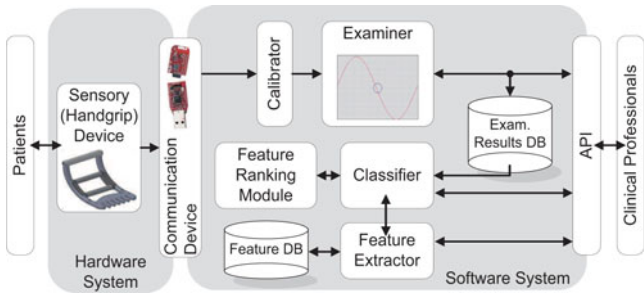

Fig. 1. Graphical overview of the proposed system.

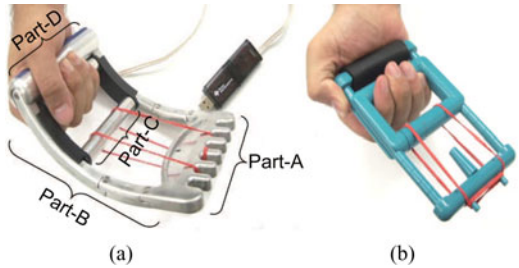

Fig. 2. (a) Physiologically designed handgrip device of the proposed system (left) and (b) the handgrip device currently in use (right).

A. Sensing Hardware

1) Handgrip Device: The handgrip device is motivated from medical devices that are currently used by clinical professionals (e.g., handgrip device in [26]), as shown in Fig. 2(b). The proposed handgrip device is illustrated in Fig. 2(a). The two cylinders bridged by the black Derlin plastic [see Part-C in Fig. 2(a)] are movable along the sideline [see Part-B in Fig. 2(a)] such that patients can grasp the device. The movable component of the handgrip device is bound to the fork-like side [see Part-A in Fig. 2(a)] of the device by a rubber band. Patients can use rubber bands of different tension forces in order to customize the maximum squeeze force in the handgrip device. Additionally, the fork-like side of the handgrip allows patients to further adjust the tension force by placing the rubber band at different widths. Finally, a force sensor is attached to Part-D in Fig. 2(a), and it measures the force generated by the grasping action.

2) Sensing Platform and Communication System: A commercial FSR force sensor (Interlink Electronics, USA) is attached to the handgrip device in order to measure the grip strength. The FSR sensor is used in the proposed system because 1) the FSR sensor responds accurately and precisely to the general range of handgrip force; and 2) the FSR shows good performance in terms of robustness [27].

In the proposed system, MSP430 (Texas Instruments, USA) is employed as the communication device, which is capable of delivering the captured sensory data in a wired or wireless manner.

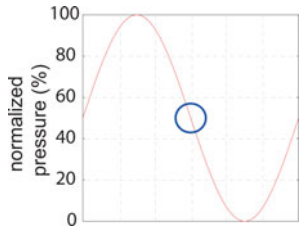

Fig. 3. Illustration of an examination using a sinusoidal waveform.

B. Software Framework

The software is composed of the front-end and the back-end software systems. The front-end software system provides a graphical interface for patients to perform the tracking examination, which will be discussed in detail in Section IV. It also provides a number of test parameters, which may change the attributes of the examination such as test duration or difficulty of the test. The back-end software system is a database system, which stores the information such that an in-depth data analysis becomes possible.

IV. Examination Procedure

The examination is designed to assess a patient's grip strength as well as a patient's ability to precisely control the strength [14], [23]. Fig. 3 illustrates an example of a tracking examination using a sinusoidal waveform. When the examination begins, the target waveform is horizontally shifted to the left at a constant speed and, as a result, the user observes a flow of the waveform within the screen. The blue circle in the middle of the screen corresponds to the level of pressure acquired from the force sensor. The blue circle is always located in the middle of the x-axis and its position in the y-axis changes according to the provided pressure. The objective of the examination is to control the grip strength to minimize the difference between the target waveform and the patient response. The software stores the target waveform, the patient's response, and various test attributes (e.g., duration or difficulty of the test) in the back-end database.

Patients may have different handgrip strengths due to various physical conditions. Therefore, the system first measures the MVC prior to the actual examination and normalizes the examination based on the MVC value for each patient. As a result, the labels on the y-axis in Fig. 3 represent the percentage of the acquired grip strength compared to the MVC measured in the calibration process (i.e., 100% in the y-axis refers to the patient's MVC).

In summary, the examination considers both the maximum strength and the preciseness of a patient's grip control as explained in [28].

V. Data Analysis

This section provides detailed discussion about 1) metrics that quantify general motor performance of patients and 2) a comparative analysis methodology that can be used to summarize the characteristics of physical symptoms of patients.

A. Comprehensive Metric to Quantify Motor Performance

In order to quantify comprehensive motor performance based on a tracking examination, various metrics have been used such as mean absolute difference (MAD) [29], root-mean- square error (RMSE) [30], mean square error (MSE) [31], mean absolute variance (MAV) [32], and the standard deviation of error (SDE) [28] between the target waveform and the patient's response. In this study, MAD and MAV are employed in order to quantify the comprehensive motor function.

B. Ailment-Specific Analysis

This section describes the in-depth data analysis method that extracts meaningful information about the characteristics of a group of patients by comparing the examination results with other subjects. For example, consider a scenario where an elderly candidate patient experiences some upper limb movement disorders and other symptoms related to a specific ailment, e.g., cerebral vascular accident (CVA) which is also known as stroke. Then, clinical professionals can perform an ailment-specific analysis on previously collected signals of patients with CVA, and reflect the results to the examination outcomes of this elderly patient. The results will allow the clinical professionals to observe 1) if the proposed system can make a clear distinction in terms of motor function between the two groups, and more importantly 2) which motor characteristics are uniquely observed among patients with CVA that help such distinction. The reason that we perform the ailment-specific analysis is because different ailments are associated with different motor characteristics, and, therefore, the motor performance of patients sharing the same ailment must be analyzed based on the specific motor characteristics of that ailment. For instance, patients with CVA often carry cognitive impairments, which result in delays between the target waveform and the patient-generated waveform due to delayed motor response. On the other hand, patients with chronic inflammatory demyelinating polyneuropathy (CIDP) only carry physical motor impairments and do not show significant delay in the results. This ailment-specific analysis allows the clinical professional to examine the candidate patient based on features that represent motor symptoms of the associated ailment for the purpose of 1) quantifying the severity of such symptoms and 2) possibly tracking the improvement over time.

In order to address this objective, the ailment-specific analysis employs the *significant-feature identification* algorithm [33], [34], which utilizes feature ranking, feature selection, and classification algorithm. The significant-feature identification algorithm performs the classification iteratively in order to observe the most frequently selected feature subsets and their associated classification accuracy.

The ailment-specific analysis begins with forming the group of signals of interest and the group of signals to be compared against, which are used as ground truth labels in order to evaluate the classification performance. Throughout this paper, the term *group of interest* (GOI) is used to generically represent the signals in which one is particularly interested to analyze. Note that this paper also uses the term *positive signals* and *negative*

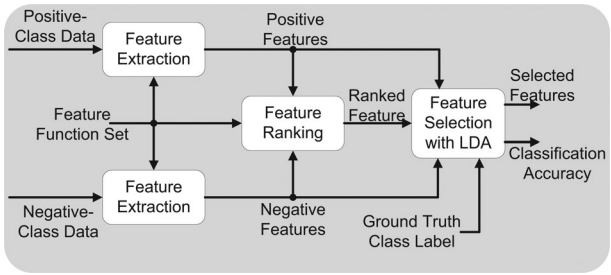

Fig. 4. Graphical overview and data flow of the analysis methodology on the *learning set*.

signals to define the signals in the GOI and the signals in the other group, respectively.

The ailment-specific analysis method employs a hold-out strategy which formulates the *learning* and the *validation* dataset in order to perform the classification iteratively [35]. The entire dataset is first divided into the *learning set* and the *validation set* using a leave-one-out cross validation (LOOCV). The *learning set* is used to extract significant features and to construct a classification model, and the *validation set* is used to evaluate the performance of the model. Then, the *learning set* is tested over the feature search space constructed by the feature ranking and feature selection algorithms. In order to do so, each element in the feature search space is evaluated based on another LOOCV within the *learning set*; the *learning set* is further divided into the *training set* and the *testing set* [35]. The feature extraction, feature ranking, and feature selection algorithms performed on the *learning set* are graphically illustrated in Fig. 4. The classification model and the signification feature set constructed by the *learning set* are finally evaluated using the *validation set*. Finally, the models and the feature sets constructed by the outer layer cross validation are further processed by *significant-feature indentification* method to extract the true significant feature set.

1) Feature Extraction: Suppose that a set of extracted features from a single examination result is represented as a horizontal array $\overline{s} = [s_1\ s_2 \cdots s_T]$, where T is the number of features. Each feature s_i is computed using a feature extraction function $f_i\left(w_g[n], w_r[n]\right)$, which is either in the time domain or frequency domain.

Representing the total number of test instances (i.e., both $learning$ and $validation$ sets) as M, a $(M \times T)$ feature matrix can be computed:

$$S = \begin{bmatrix} \overline{s}^1 \\ \overline{s}^2 \\ \vdots \\ \overline{s}^M \end{bmatrix} = \begin{bmatrix} s_1^1 & s_2^1 & \cdots & s_T^1 \\ s_1^2 & s_2^2 & \cdots & s_T^2 \\ \vdots & & \ddots & \vdots \\ s_1^M & s_2^M & \cdots & s_T^M \end{bmatrix} \tag{1}$$

$$= \begin{bmatrix} \overline{s}_1 & \overline{s}_2 & \cdots & \overline{s}_T \end{bmatrix} \tag{2}$$

where $\overline{s}^j$ with $j \in [1, M]$ is a horizontal array of features, and $\overline{s}_i$ with $i \in [1, T]$ is a vertical array composed of values of a feature $f_i(\cdot)$ computed from the entire signals.

2) Feature Ranking and Feature Selection: As explained earlier, the feature ranking and feature selection algorithms are performed on the *learning set*. The reason that feature ranking and feature selection techniques are employed are as follows. First, given a predefined set of features $\overline{s}$, not all of these features play an important role in classifying a certain GOI. This may lead to a problem during the classification process that a collection of many useless features can be accumulated to overwhelm some useful features. Second, it is more computationally efficient since it filters out features that are less useful. Finally, information about the ranks of features according to the level of contributions in the classification process is valuable to us because features with higher rank can be defined as physical symptoms found only in that GOI.

The proposed system employs the estimated Pearson correlation coefficients to rank the features according to the level of correlation to the class labels (i.e., positive or negative signals). The Pearson correlation coefficient for a feature f_i, can be estimated using

$$R(i) = \frac{\sum_{j=1}^{M'} \left(s_i^j - E(\overline{s}_i)\right)\left(y^j - E(\overline{y})\right)}{\sqrt{\sum_{j=1}^{M'} \left(s_i^j - E(\overline{s}_i)\right)^2 \sum_{j=1}^{M'} \left(y^j - E(\overline{y})\right)^2}} \tag{3}$$

where y^j with $j \in [1, M']$ represents the class of the signal j (i.e., $+1$ for positive and -1 for negative class signal). M' represents the size of the *learning set* (i.e., $M' = M - 1$ since LOOCV is applied). $E(\cdot)$ represents a function computing the mean value of the input vector. Then, we use $R(i)^2$ as a feature ranking criterion that estimates goodness of linear fit of an individual feature to the class vector $\overline{y}$ [36].

Given the rank of all features, the well-known *forward selection* strategy is used to construct the search space, which starts with the highest ranked feature and gradually adds a feature that is the next highest. Then, the size of the search space is reduced to $T - 1$. Each feature subset is evaluated using linear discriminant analysis (LDA), and the feature subset with the highest averaged classification accuracy is selected.

3) Identifying Significant Features: When the best performing feature subset is selected, the *learning set* is projected onto the selected features and the classification model is trained. Then, the *validation set* is classified and evaluated using LDA. The classification accuracy is computed by averaging the number of correctly classified instances over M validation sets (created by the outer LOOCV) using LDA. Moreover, the algorithm produces M feature subsets that are selected by the feature selection technique. In order to investigate the significant feature subsets, we compute the followings over the cross validations: 1) the most frequently appearing feature subset; 2) the top K features for the accumulated ranking score; and 3) the associated classification accuracy. Intuitively, the more frequently selected feature subset carries more relevant information about the patients that we are interested [34].

VI. Validation

A. Clinical Trial

We have conducted a clinical trial at St. Vincent Medical Center (Los Angeles, CA, USA). A total of 16 subjects participated in this clinical trial and provided 78 examination instances. Among the participating subjects, 12 of the study's subjects were patients (mean age of 70.5 years with a standard deviation

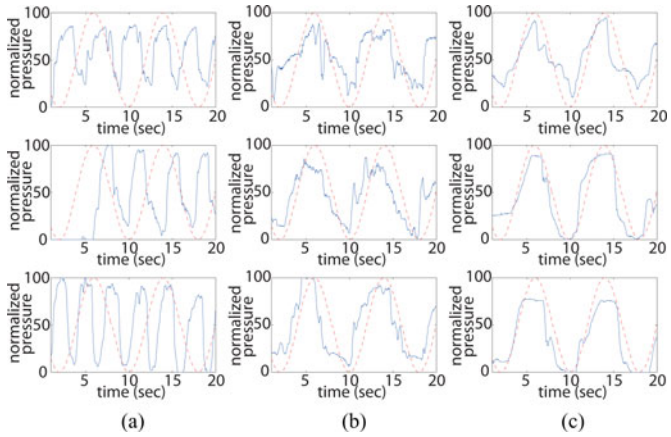

Fig. 5. Randomly selected sample signals of subjects with various conditions. The three signals in column (a) belong to patients with CVA. The signals in column (b) belong to patients with CIDP. The signals in column (c) are sample signals of healthy subjects.

of 10.5), and they produced a total of 67 examination results. The remaining four subjects were healthy individuals (mean age of 64.3 years with a standard deviation of 12.1) and the data collected from these subjects resulted in 11 examination instances. All patients had motor deficits in their upper limbs and they were examined prior to any operational treatments. All subjects performed the examination while he/she sat upright, had the elbow flexed 90° with the arm close to the body, and had the wrist and forearm resting on a table. Prototype software that was designed from our laboratory was used to perform the examination. The user interface provides real-time visual feedback to the subject to perform motor movements consistent with the desirable waveform. The interface is developed in C# .NET and it communicates with the back-end server, which is an SQL database.

The 16 subjects that participated in the clinical study were grouped based on their primary medical problems. For instance, if a patient was actively diagnosed for CVA, that patient was assigned to the CVA group. This resulted in the formation of two primary ailment groups: 1) a group of patients with CVA and 2) a group of patients with CIDP. These GOIs will be the focus of our experimental validation for the rest of this paper.

These two groups are chosen such that each ailment group can be analyzed with sufficient data that can be used for both learning and validation. For example, the number of examination results for the patients with CVA was 17 and the number of results for patients with CIDP was 24. The rest of the patients were diagnosed with various ailments with upper limb deficits such as Parkinson's disease and intracerebral hemorrhage but were eliminated from the analysis due to the relatively small number of signals (e.g., we had only one patient diagnosed with each of these ailments).

Fig. 5 illustrates sample examination results of the two ailment groups and the healthy subjects that we consider in this analysis. As illustrated, the examination results provide clear visual distinction between the health subjects and patients. CVA patients seem to exhibit delayed movements often having difficulties of coordinating the speed of the moving sinusoidal waveform. It may be a result of both physical and cognitive problems, which are common symptoms of CVA. The signals of CIDP have high level of noise compared to those of healthy subjects, which may be a result of a tremor effect. On the other hand, the signals of healthy subjects are smooth and well correlated to the target waveform.

B. Features Used in the Analysis

This section presents features that are used in the data analysis. A total of 45 candidate feature functions are defined, where the first 36 feature functions are in the time-domain and the following 9 feature functions are in the frequency domain.

The first time-domain feature extraction function, denoted as f_1, represent MAD between the target waveform and the waveform generated by the subject. This function provides the overall level of performance in term of preciseness. f_2 computes the maximum instantaneous change in magnitude of the subject-generated waveform in order to investigate how well a subject manipulates the grip strength. f_3 computes the minimum time required for the subject-generated waveform to cross the target waveform from the time that the examination begins in order to investigate the subject's recovery time from deviation. The fourth time-domain function f_4 computes the total number of intersections of two waveforms in order to investigate a subject's ability to control the grip strength to stay near the target waveform. f_5 investigates the number of changes in the sign of the slope of the patient-generated waveform in order to correlate the examination results to possible tremor effects. f_6 and f_7 compute the number of times that the subject-generated waveform crosses horizontal lines at magnitude $y = 50\%$ and $y = 25\%$, respectively. The time-domain functions from f_8 to f_{22} are constructed as the following. 20 s-long waveforms generated by subjects are quantized into 15 segments of uniform length (i.e., each segment contains the data of 20/15 s). Then, f_8 to f_{22} contain the mean values of the magnitude of these segments. These quantized segments are used to evaluate the changes in grip strength over time. Furthermore, the time-domain functions from f_{23} to f_{36} compute the difference in mean magnitude of the two neighboring segments. These features are used to evaluate how fast the grip strength of a patient changes over time. The frequency-domain functions used in this analysis are computed as the following. The first frequency-domain function f_{37} computes the average difference in magnitude between the DFT of the target waveform and the DFT of the subject-generated waveform over all the possible frequency range. The frequency-domain functions from f_{38} to f_{45} divide the frequency range from 0 to 16 Hz into 8 segments of uniform length (i.e., 2 Hz), and compute the spectrum energy for each segment in order to investigate the tremor effect at various frequency ranges.

C. Comprehensive Quantification of Motor Performance

This section presents the results of quantification of motor performance based on the metrics discussed in Section V-A. The results of the two groups of major ailments are compared against the results of healthy subjects and they are illustrated in Fig. 6. The comparative results of the two ailment groups to the healthy group show that there exist significant degradations in motor performance in the ailment groups. These results show

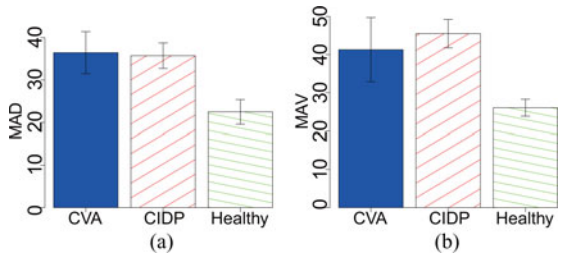

Fig. 6. (a) MAD and (b) MAV for three groups: Patients with CVA, patients with CIDP, and healthy subjects.

that the proposed system can be used for a preliminary screening device to quantify grip motor performance and compare the results against healthy subjects. This further implies that 1) the system may distinguish patients with upper limb deficits and 2) the system provides a reference motor performance of subjects in a healthy physical status such that the improvement of a patient's motor capacity can be tracked.

D. Ailment-Specific Analysis Results

This section presents the data analysis results when the signals of patients with CVA and CIDP are compared against various groups of subjects: 1) all patients without the ailment; 2) healthy subjects; and 3) the union of 1) and 2) (i.e., all subjects without the ailment). For example, when the positive-class signals are defined as the signals of patients with CVA, the negative-class signals are defined as 1) signals of patients without CVA (i.e., excluding healthy subjects); 2) signals of healthy subjects; and 3) combined signals of patients without CVA and healthy subjects. In this paper, we generically use the term *classification instances* for these three different positive and negative class combinations and label each instance as 1) a non-CVA instance; 2) a healthy subject instance; and 3) a combined instance.

1) CVA Detection: The data analytic results are summarized in Table I. The sixth and the seventh columns represent the number of the selected features and their labels, respectively. The last column represents the top single feature with the highest accumulated ranking score (i.e., $K = 1$ in Section V-B3). The corresponding classification accuracies for the *non-CVA patients instance*, *healthy subjects instance*, and the *combined instance* are 94.64%, 95.00%, and 92.54%, respectively. These high classification accuracies show that the physiological signals produced by the proposed system contain ailment-specific information, which can be further interpreted as the motor characteristics of that ailment. For CVA patients, interestingly, the most frequent features for all three classification instances are identical (i.e., f_{36} and f_{39}). Fig. 7 illustrates the empirical distributions of the three features, which show clear separation between the positive (blue) and the negative (shaded red) classes.

Feature f_{36} represents the MAD of the last two temporal segments as was explained in the previous section, and the results in Fig. 7 show that CVA patients have relatively higher values compared to the rest of the subjects. Thus, it may help the physicians to see that the selected patients may dramatically lose the preciseness of their grip control (or simply the grip strength) as the test proceeds toward the end. Moreover, feature f_{39} represents the spectrum energy of the patient response at the frequency range between 2 to 4 Hz, and Fig. 7 shows that the selected patients have relatively low spectral energy at this frequency range.

2) CIDP Detection: When the positive signals are defined as the signals of CIDP patients and compared against *non-CIDP patients instance*, *healthy subjects instance*, and the *combined instance*, the classification accuracies are 91.07%, 91.42%, and 85.07%, respectively. According to Table I, a number of interesting observations are made on the results for CIDP patients.

First, feature f_{32} is found in all instances and always ranked the highest. It implies that this feature best represents the characteristic of the signals of CIDP, which is selected in the most frequent feature subsets regardless of the definition of the negative class.

Second, the most frequent feature set for the *combined instance* seems to be the union of the feature sets of the rest of the two instances. For example, f_{13} and f_{26} are found in the *patients without CIDP* instance and f_{27} and f_{11} are found in the *healthy subject* instance. This may result from the fact that the signals of the *combined instance* is the union of signals of the rest of the two instances.

f_{36} represents the difference in the average magnitude errors of the last two temporal segments, and according to our investigation, CIDP patients have relatively low value of f_{36}. This result shows that the selected patients can maintain the grip preciseness (or grip strength) until the very end of the examination as compared to the rest of the subjects. Moreover, f_{13} indicates the MAD between the target waveform and the patient's response at the sixth temporal segment, where it contains a minimal point in sinusoidal waveform. The empirical distribution indicates that CIDP patients have relatively low error rates in that segment. More interestingly f_{27} which is selected as one of the top ranked features, shows that the difference in MAD between the fifth and sixth temporal segments is relatively high. These results indicate that CIDP patients lose their grip muscle control when the amplitude of the waveform starts to increase. Thus, patients may have trouble with the required grip strength.

E. Patient-Independent Ailment-Specific Analysis

Patient-independent classification involves validating the signals of patients that are excluded from those being used to train the classification model. (e.g., *learning* on CVA patient #1, #2, #3 and *validating* on CVA patient #4). This preliminary study is particularly important to investigate if the system can provide ailment specific information without the previous history of a new patient. Furthermore, it demonstrates the robustness and independence of the proposed system to the data on which the system is initially constructed. In this experiment, four different classification instances are considered as shown in Table II. For each classification instance, the classification accuracy is averaged among all *learning-validation* dataset combinations (i.e., leave-one-patient-out cross validation).

The selected features were different among different *learning-validating* set combinations within a classification instance. For the *CVA versus Healthy Subject* instance, the number of features in the most frequent feature subsets for the four combinations were 2, 2, 3, and 3. In order to investigate the most

TABLE I
SUMMARY OF THE EXPERIMENTAL RESULTS WHEN THE POSITIVE CLASS IS DEFINED AS (I) CVA AND (II) CIDP

Positive Class	Negative Class	Classification Accuracy	True Positive	True Negative	Size of most Frequent Subset	Most Frequent Subset Features	Top Ranked Feature
CVA	non-CVA Patients	0.9464	0.8889	0.9574	2	f_{36}, f_{39}	f_{36}
	Healthy subjects	0.9500	0.8889	1.0000	2	f_{39}, f_{36}	f_{36}
	Combined	0.9254	0.7778	0.9483	2	f_{36}, f_{39}	f_{36}
CIDP	non-CIDP Patients	0.9107	0.9167	0.9063	7	f_{32}, f_{14}, f_{13}, f_{24} f_{36}, f_{26}, f_{45}	f_{32}
	Healthy subjects	0.9142	1.0000	0.7200	6	f_{32}, f_{25}, f_{27} f_{11}, f_{2}, f_{19}	f_{32}
	Combined	0.8507	0.8333	0.8605	10	f_{32}, f_{13}, f_{27}, f_{36}, f_{24} f_{11}, f_{8}, f_{14}, f_{26}, f_{45}	f_{32}

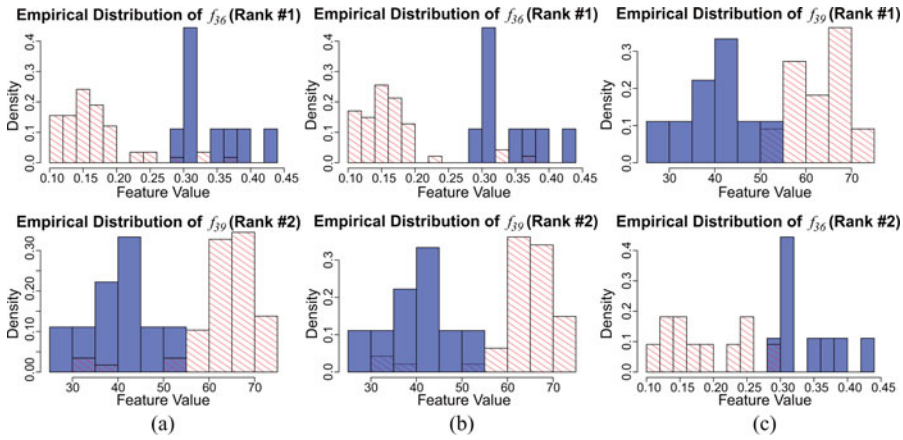

Fig. 7. Empirical distribution of the selected features when the signals of CVA patients are compared against (a) combined group (f_{36} and f_{39}), (b) patients with CVA (f_{36} and f_{39}), and (c) healthy subjects (f_{39} and f_{36}).

TABLE II
SUMMARY OF THE EXPERIMENTAL RESULTS ON PATIENT INDEPENDENT AILMENT CLASSIFICATION

Positive Class	Negative Class	Classification Accuracy	True Positive	True Negative
CVA	Healthy	0.9167	0.9091	0.9231
Healthy	CVA	1.0000	1.0000	1.0000
CIDP	Healthy	0.7610	0.8276	0.5385
Healthy	CIDP	0.8542	0.8462	0.8276

frequent feature subsets of this patient-independent classification results, the following analysis has been performed.

First, the top ten ranked features from each *learning-validating* combination have been extracted. The reason that we observe the top ten features (out of 45 features) is to verify that relatively small number of motor characteristics can generalize the signals of the same ailment through patient independent analysis. Then, the features that have appeared in all of those four top ten feature sets are observed. These features for CVA patients are $F_{\text{ind}} = [f_{39}\ f_{36}\ f_{43}\ f_{42}\ f_{38}\ f_{37}]$. In other words, the same six features are shared among the top ten ranked features when the classification is performed in a patient-independent way. This is a strong evidence that similar motor characteristics are observed among patients with CVA.

Next, the top ten ranked features are extracted from the results of the *CVA versus Healthy Subject* instance from Section VI-D (i.e., the result shown in the third row of Table I). The top ten ranked features were $F_{\text{dep}} = [f_{39}\ f_{36}\ f_{43}\ f_{42}\ f_{37}\ f_{46}\ f_{38}\ f_{45}\ f_{40}\ f_{16}]$. It can be easily observed that $F_{\text{ind}} \subset F_{\text{dep}}$, that is, similar features are observed across all the patients with CVA. Note also that features f_{39} and f_{36}, which were the selected features in Section VI-D, also appeared as the top two features for all *learning-validating* combinations in the patient independent classification.

Similar observations were made with CIDP patients.

VII. DISCUSSION AND FUTURE WORK

Our main goal in this study was to demonstrate the efficiency of the presented handgrip device and its back-end data analysis for diagnosis of hand movement deficits. Given that clinical data collection is an expensive and time-consuming process, we decided to validate our system based on a pilot clinical trial with limited patient population. For this, we performed an in-depth data analysis on the grip tracking signals collected from 16 subjects at St. Vincent Medical Center (Los Angeles, CA, USA) and have achieved promising results. We believe that this proof-of-concept opens new routes for us to apply the proposed methods to a larger population.

With larger datasets, the system also can be configured to consider varying levels of granularity in the levels of motor disorders. For example, the NIH Storke Scale (NIHSS) is a widely used tool that classifies the level of impairment caused by a stroke [37]. The proposed measurement model can be independently constructed on each of these classes, which allows for an accurate analysis of motor symptoms at different levels of severity.

The validation of the system to reflect the changes in motor performance before and after a medical treatment (e.g., operational surgery) is also an important issue to be addressed. In an ongoing clinical trial, we are conducting a longitudinal study on a larger patient population through a collaboration with the UCLA Department of Neurosurgery, which includes patients with spinal cord injury in cervical region.

VIII. Conclusion

In this paper, we introduce a portable handgrip device and its associated data analysis method, which together quantify hand-movement performance for patients with movement disorders. Two data analysis methods are discussed: a comprehensive metric for quantifying motor performance and an ailment-based comparative analysis. We showed that the comprehensive metric that quantifies motor performance can successfully distinguish patients with hand–motor deficits from healthy subjects. More importantly, the subset features that contribute the most to these classification instances are discussed in detail in order to provide intuitive analysis on ailment conditions. This study enables new opportunities for accurate quantification of an individual's ailment condition, disease severity, and specific physiological symptoms.

References

[1] F. Alarcon, J. Zijlmans, G. Duenas, and N. Cevallos, "Post-stroke movement disorders: Report of 56 patients," *J. Neurol. Neurosurg. Psychiatry*, vol. 75, no. 11, pp. 1568–1574, 2004.

[2] M. Morris, "Movement disorders in people with parkinson disease: A model for physical therapy," *Phys. Ther.*, vol. 80, no. 6, pp. 578–597, Jun. 2000.

[3] J. Conomy, "Disorders of body image after spinal cord injury," *Neurology*, vol. 23, no. 8, pp. 842–850, 1973

[4] E. Critchley, "Speech disorders of parkinsonism: A review," *J. Neurol. Neurosurg. Psychiatry*, vol. 44, no. 9, pp. 751–758, 1981.

[5] R. Jafari, D. Jindrich, V. Edgerton, and M. Sarrafzadeh, "CMAS: Clinical movement assessment system for neuromotor disorders," presented at the IEEE BioCase, London, U.K., Nov. 2006

[6] A. Fugl-Meyer, L. Jaasko, S. Olsson, and S. Steglind, "The post-stroke hemiplegic patient—Part1: A method for evaluation of physical performance," *Scand. J. Rehabil. Med.*, vol. 7, no. 1, pp. 13–31, 1975

[7] E. Hudyma and G. Terlikowski, "Computer-aided detecting of early strokes and its evaluation on the base of ct images," in *Proc. Int. Multiconf. Computer Science and Information Technology*, Busan, South Korea, Nov. 2008, pp. 251–254.

[8] D. Gladstone, C. Danells, and S. Black, "The Fugl–Meyer assessment of motor recovery after stroke: A critical review of its measurement properties," *Neurorehabil. Neural Repair*, vol. 16, no. 3, pp. 232–240, 2002.

[9] C. Dumont, M. Popovic, T. Keller, and R. Sheikh, "Dynamic force-sharing in multi-digit task," *Clin. Biomech.*, vol. 21, no. 2, pp. 138–146, Feb. 2006.

[10] P. Raghavan, E. Petra1, J. W. Krakauer, and A. M. Gordon, "Patterns of impairment in digit independence after subcortical stroke," *J. Neurophysiol.*, vol. 95, no. 1, pp. 269–278, 2006.

[11] S. I. Lee, J. Woodbridge, A. Nahapetian, and M. Sarrafzadeh, "MARHS: Mobility assessment system with remote healthcare functionality for movement disorders," presented at the ACM International Health Informatics 2012, Miami, FL, USA, Jan. 2012

[12] L. H. Jakobsen, I. K. Rask, and J. Kondrup, "Validation of handgrip strength and endurance as a measure of physical function and quality of life in healthy subjects and patients," *Nutrition*, 2009.

[13] W. Memberg and P. Crago, "Instrumented objects for quantitative evaluation of hand grasp," *J. Rehabil. Res. Development*, vol. 34, no. 1, pp. 82–90, Jan. 1997.

[14] G. Kurillo, M. Gregoric, N. Goljar, and T. Bajd, "Grip force tracking system for assessment and rehabilitation of hand function," *J. Technol. Health Care*, vol. 13, no. 3, pp. 137–149, 2005.

[15] R. Getachew, S. I. Lee, J. Kimball, A. Yew, N. Ghalehsari, B. Paak, D. C. Lu, and M. Sarrafzadeh, "Utilization of a novel digital measurement tool for quantitative assessment of upper extremity motor dexterity in cervical spondylotic myelopathy," presented at the 29th Annu. Meet. AANS/CNS, Phoenix, AZ, USA, Mar. 2013.

[16] S. I. Lee, R. Getachew, J. Kimball, A. Yew, N. Ghalehsari, B. Paak, J. Garst, D. C. Lu, and M. Sarrafzadeh, "Utilization of a novel digital device and an analytic method for accurate measurement of upper extremity motor function," presented at the 81st Annu. Scientif. Meet., New Orleans, LA, USA, Apr. 2013.

[17] S. I. Lee, H. Ghasemzadeh, A. Yew, R. Getachew, J. Kimball, N. Ghalehsari, B. Paak, J. Garst, M. Razaghy, D. C. Lu, and M. Sarrafzadeh, "Objective assessment of spastic hand hypertonia using a novel digital device," presented at the 20th IAGG World Congr. Gerontol. Geriatr., Seoul, Korea, Jun. 2013.

[18] S. I. Lee, H. Ghasemzadeh, B. J. Mortazavi, A. Yew, R. Getachew, M. Razaghy, N. Ghalehsari, B. H. Paak, J. H. Garst, M. Espinal, J. Kimball, D. C. Lu, and M. Sarrafzadeh, "Objective assessment of overexcited hand movements using a lightweight sensory device," in *Proc. IEEE Body Sensor Networks*, MIT, Cambridge, MA, USA, May 2013, pp. 1–6.

[19] M. Morris, "Movement disorders in people with parkinson's disease: A model for physical therapy," *Phys. Ther.*, vol. 80, pp. 578–597, 2000.

[20] J. Hermsdorfer, E. Hagl, D. A. Nowak, and C. Marquardt, "Grip force control during object manipulation in cerebral stroke," *Clin. Neurophys.*, vol. 114, pp. 915–929, 2003.

[21] A. Sunderland, D. Tinson, L. Bradley, and R. L. Hewer, "Arm function after stroke. An evaluation of grip strength as a measure of recovery and a prognostic indicator," *J. Neurol. Neurosurg. Psychiatry*, vol. 52, pp. 1267–1272, 1989.

[22] I. Merkies, P. Samijn, J. P. Samijn, F. Mech, K. V. Toyka, and P. A. van Doorn, "Assessing grip strength in healthy individuals and patients with immune-mediated polyneuropathies," *Muscle Nerve*, vol. 52, pp. 1393–1401, 2000.

[23] G. Kurillo, A. Zupan, and T. Bajd, "Force tracking system for the assessment of grip force control in patients with neuromuscular diseases," *Clin. Biomech.*, vol. 19, pp. 1014–1021, 2004.

[24] W. Sharp and K. Newel, "Coordination of grip configurations as a function of force output," *J. Motor Behav.*, vol. 32, pp. 73–82, 2000.

[25] R. Wenzelburger, F. Kopper, A. Frenzel, H. Stolze, S. Klebe, A. Brossmann, J. Kuhtz-Buschbeck, M. Glge, M. Illert, and G. Deuschl, "Hand coordination following capsular stroke," *Brain*, vol. 128, pp. 64–74, 2005.

[26] C. Waggoner and R. LeLieuvre, "A method to increase compliance to exercise regimens in rheumatoid arthritis patients," *J. Behav. Med.*, vol. 4, no. 2, pp. 191–201, Jun. 1981.

[27] F. Vecchi, C. Freschi, S. Micera, A. M. Sabatini, P. Dario, and R. Sacchetti, "Experimental evaluation of two commercial force sensors for applications in biomechanics and motor control," presented at the Int. Functional Electric Stimulation Society Conf., Aalborg, Denmark, Jun. 2000.

[28] R. Jones, *Mesurement of Sensory-Motor Control Performance Capacities: Tracking Tasks*. Boca Raton, FL, USA: CRC Press, 2000.

[29] E. Poulton, *Tracking Skill and Manual Control*. New York, NY, USA: Academic, 1974.

[30] N. O'Dwyer and P. Neilson, *Adaptation to a Changed Sensory-Motor Relation: Immediate and Delayed Parametric Modification*. Champaign, IL, USA: Human Kinetics, 1995.

[31] P. Neilson, M. Neilson, and N. O'Dwyer, "What limits high speed tracking performance?," *Human Movement Sci.*, vol. 12, pp. 85–109, 1993.

[32] P. Neilson and M. D. Neilson, "Influence of control-display compatibility on tracking behavior," *Quart. J. Exp. Psychol*, vol. 32, pp. 125–135, 1980.

[33] A. Sung and S. Mukkamala, "Identifying important features for intrusion detection using support vector machines and neural networks," in *Proc. Symp. Appl. Internet*, 2003, pp. 209–216.

[34] C. Spence and P. Sajda, "The role of feature selection in building pattern recognizers for computer-aided diagnosis," *Proc. SPIE*, vol. 3338, pp. 1434–1441, Jun. 1998.

[35] R. Bellazzi and B. Zupan, "Predictive data mining in clinical medicine: Current issues and guidelines," *Int. J. Med. Inform.*, vol. 77, no. 2, pp. 81–97, 2008.

[36] I. Guyon and A. Elisseeff, "An introduction to variable and feature selection," *J. Mach. Learn. Res.*, vol. 3, pp. 1157–1182, Mar. 2003.

[37] V. Hage, "The NIH stroke scale: A window into neurological status," *Nurse.Com Nursing Spectrum (serial online)*, vol. 24, pp. 44–49, 2011.

Authors, photographs and biographies not available at the time of publication.